

1 **Aqueous Film Forming Foam and Associated Perfluoroalkyl Substances Inhibit Methane**  
2 **Production and Co-contaminant Degradation in an Anaerobic Microbial Community**

3

4 *Nicole J.M. Fitzgerald<sup>1,2</sup>, Hanna R. Temme<sup>1</sup>, Matt F. Simcik<sup>3</sup>, Paige J. Novak<sup>1\*</sup>*

5

6

7 <sup>1</sup>Department of Civil, Environmental, and Geo- Engineering, University of Minnesota, 500  
8 Pillsbury Drive SE, Minneapolis, Minnesota 55455

9

10 <sup>2</sup>Current Address: Department of Civil and Environmental Engineering, Colorado School of  
11 Mines 1500 Illinois Street, Golden, CO 80401

12

13 <sup>3</sup>School of Public Health, University of Minnesota, 420 Delaware St. S.E. Minneapolis, MN  
14 55455

15

16

17

18 \*Co-corresponding authors to whom correspondence should be addressed: NJMF: phone: 847-  
19 791-2844, email: [nicolefitzgerald@mines.edu](mailto:nicolefitzgerald@mines.edu); PJN: phone 612-626-9846, email:

20 [novak010@umn.edu](mailto:novak010@umn.edu)

21

22

23

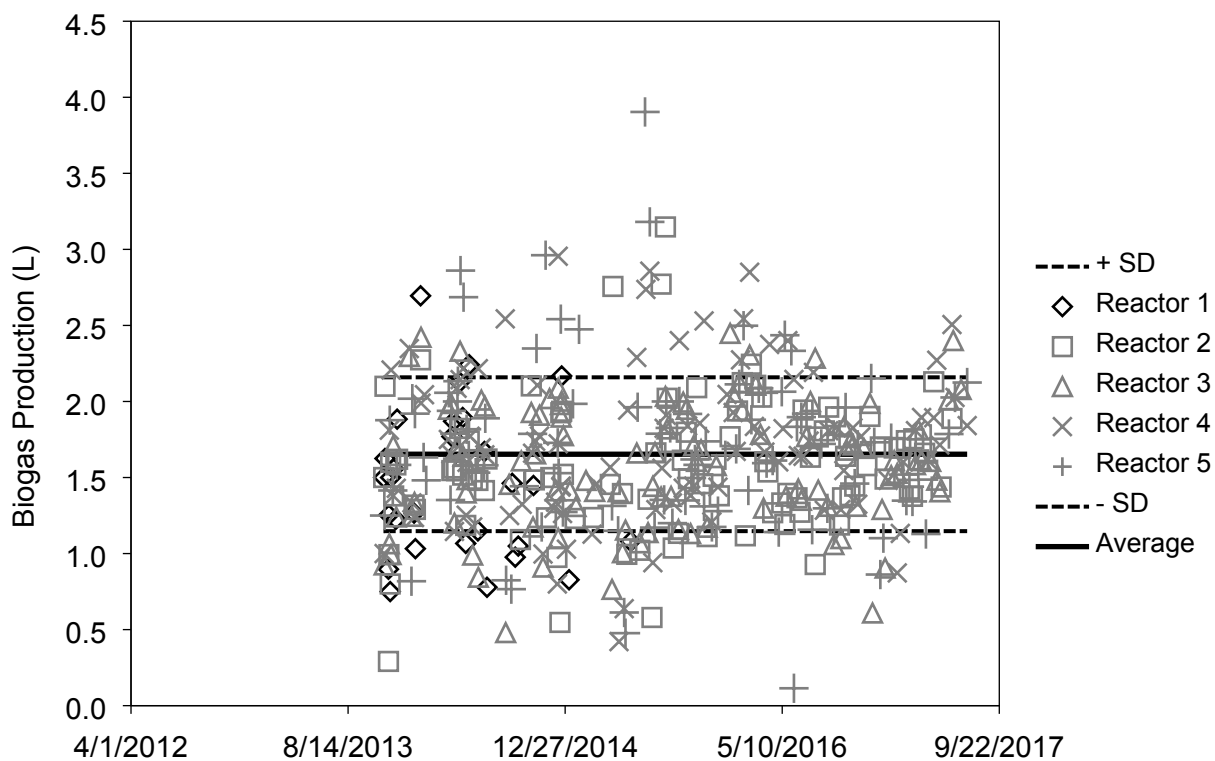
24 **METHODS**

25 **Microbial Culture**

26 The feed sludge (thickened waste activated and primary sludge) was obtained from the  
27 Empire Wastewater Treatment Plant (Farmington, MN) and collected in a plastic carboy.

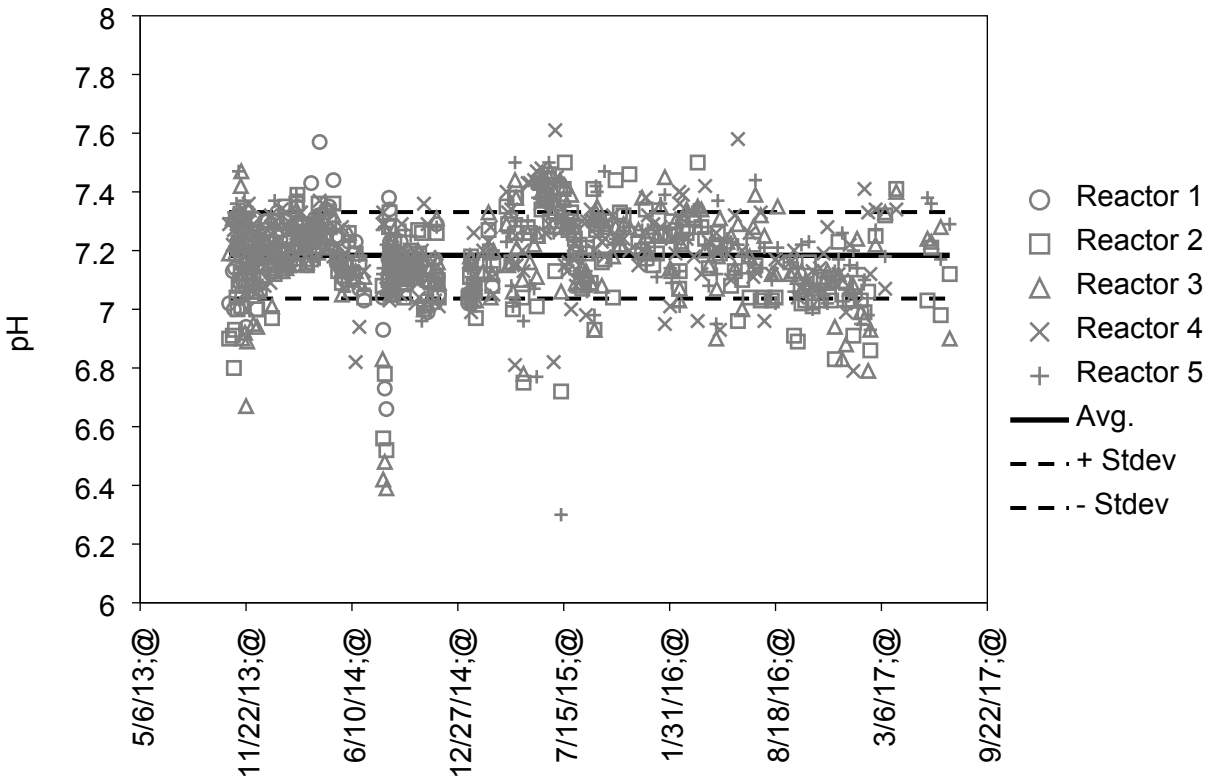
28 Performance of source culture is shown in Figures SI.1 and SI.2.

29



30 **Figure SI.1. Biogas production from source reactors. All reactors are identical.**

31



32

33 **Figure SI.2. pH in source reactors. All reactors are identical.**

34

35 **Microbial Analysis**

36 ***Illumina Sequencing.*** Samples were taken for DNA analysis in 1 ml aliquots, pelleted,  
 37 and frozen immediately at -20°C until DNA was extracted. The Fast DNA extraction kit (MP  
 38 Bio) was used according to the manufacturer’s instructions. Extracted DNA was stored at -20°C  
 39 until analysis. Illumina sequencing of the 16S rRNA gene was completed by the University of  
 40 Minnesota Genomics Center (UMGC). The V4-V6 region of the 16S rRNA gene was amplified  
 41 with primers F- GTGCCAGCMGCCGCGGTAA and R- GACRRCATGCANACCT and  
 42 sequenced using Illumina MiSeq paired end sequencing (2x300). Initial quality filtering of the  
 43 data was completed with the Gopher pipeline available on the Minnesota Supercomputing  
 44 Institute (MSI) and is available for public use (Gopher pipelines by John Garbe; accessed 7/8/19,

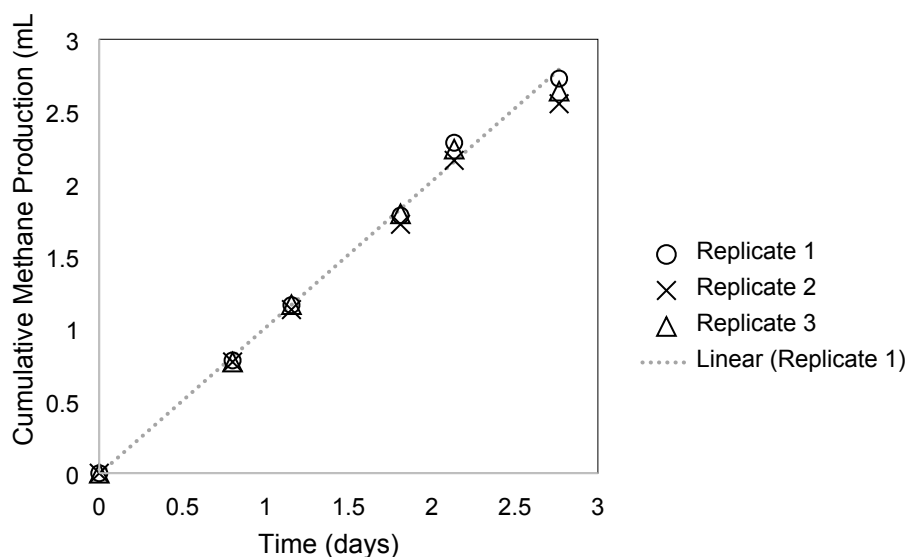
45 <https://bitbucket.org/jgarbe/gopher-pipelines/src/default/>). Trimmomatic was used for primer  
46 removal and quality filtering, trimming the reads when the average read quality dropped below  
47 25 over a 4 base pair window. The forward and reverse reads were concatenated. The samples  
48 were then rarified to the sample with the least number of quality filtered reads. Denovo OTU  
49 picking was completed with QIIME using the Uclust algorithm and 97% similarity. Taxonomy  
50 was assigned with QIIME using the SILVA database. Whole community data and data from  
51 which the *Archaea* were excluded (*i.e.*, *Bacteria* only) were both analyzed; results were very  
52 similar and therefore suggested that the *Archaea* were not adequately represented with the  
53 Illumina primers selected. Therefore, only the community data for *Bacteria* were considered in  
54 our analysis. Beta diversity analysis was completed in R with the Phyloseq package. The beta  
55 diversity between the samples was calculated using Bray Curtis. R was then used to complete a  
56 hierarchal clustering of the samples.

57 ***Quantitative Polymerase Chain Reaction.*** To quantify methanogens, primers specific for  
58 the 16S rRNA gene of methanogens were used (630 F- GGATTAGATACCCSGGTAGT and  
59 803R –GTTGARTCCAATTAAACCGCA)(1). This targeted an approximate 175 bp region of  
60 the 16S rRNA gene and was verified in other publications(1–3). Each qPCR reaction contained  
61 1X SYBR green MasterMix (Bio-Rad Laboratories), 100 nM of each primer (IDT), 1 mg/L  
62 BSA, and 1 µl of purified DNA. All qPCR analysis was performed on a Biorad CFX Connect  
63 Real-Time System. The general qPCR cycle was an initial denaturation at 95°C for 1 min  
64 followed by 40 cycles of: 95°C for 15 s and 60°C for 1 min. A melt curve analysis was  
65 completed at the end of each run for quality control. A 10-fold dilution standard curve ranging  
66 from 10<sup>9</sup> to 10<sup>0</sup> was used to quantify the number of gene copies in each sample. Standards were  
67 purchased from IDT as gblocks based on the 16S rRNA gene sequence of *Methanobrevibacter*

68 *smithii* (Genbank accession no. U55234). The standard curve was linear from  $10^9$  to  $10^1$  and the  
69 limit of detection was determined to be  $10^1$ . The qPCR efficiency was 106% and the standard  
70 curve had an  $R^2$  of 0.996. No template controls were used as qPCR negative controls and nothing  
71 was detected from these samples. To determine whether differences in methanogen numbers  
72 between samples were significant, t-tests were performed with P-values corrected via the  
73 Tukey's correction.

#### 74 **Data Analysis**

75 **Toxicity.** The rate of methane production was calculated for each bottle by linear  
76 regression of the data from the first three days of the experiment. Rates were then averaged  
77 among the triplicate bottles. Methane production during this time frame was consistently linear  
78 as depicted in Figure SI.3.



79

80 **Figure SI.3. Linear regression of replicate control bottles during the first three days of an experiment.**

81

82

83

84

## 85 RESULTS & DISCUSSION

86 Table SI.1 shows the *P*-values obtained during statistical comparisons (t-tests) of the rate  
87 of methane production in the PFAS-amended treatments compared to the no-PFAS control.  
88 Outliers were removed with Grubbs' correction with  $\alpha=0.05$ . The Tukey correction was used to  
89 correct *P*-values for multiple comparisons. Some experiments were repeated; therefore, in some  
90 cases multiple *P*-values are presented.

91  
92 **Table SI.1. *P*-values corrected for multiple comparisons and obtained from statistical comparisons between**  
93 **the rate of methane production in PFAS-amended treatments and the no-PFAS control treatments (Figure**  
94 **SI.3). Some experiments were repeated, hence multiple *P*-values are presented.**

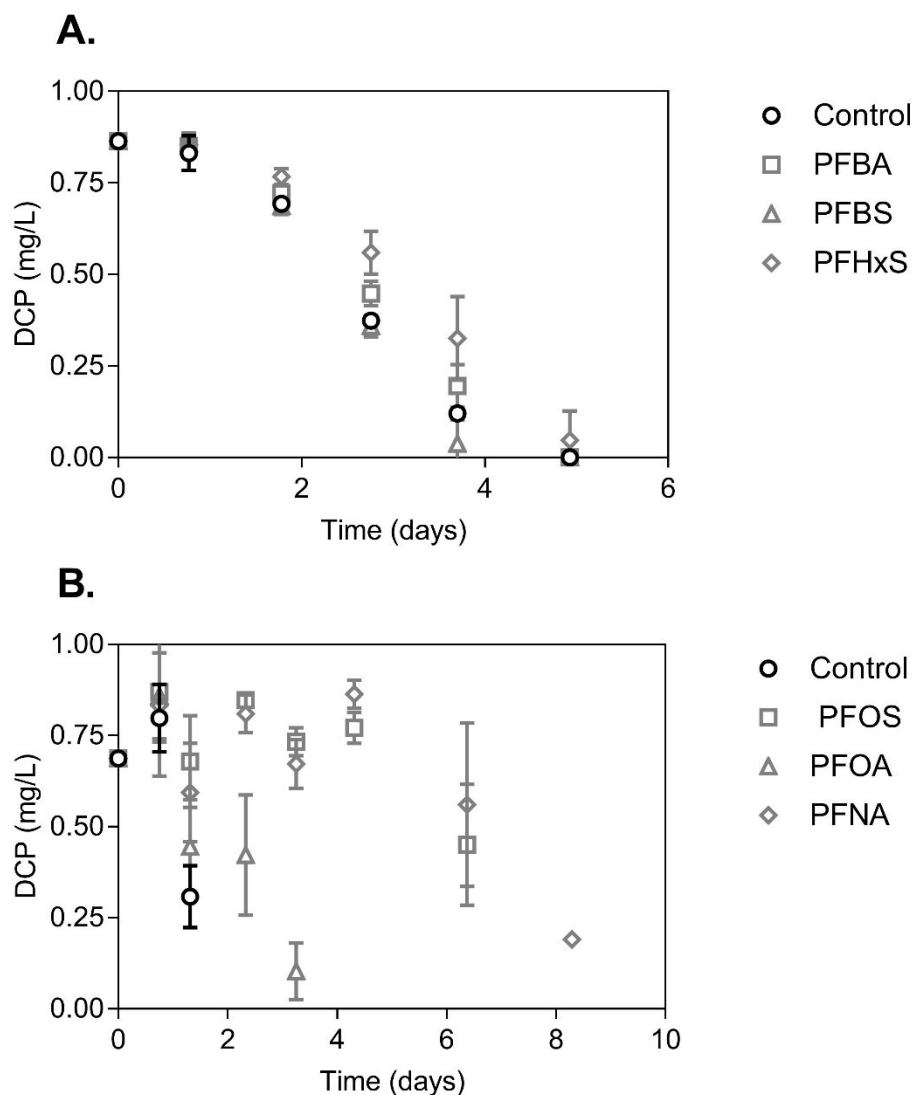
95

Treatment	<i>P</i> -value
<i>Carboxylates</i>	
PFBA (3C)	>0.99, 0.91,
PFOA (7C)	>0.99
PFNA (8C)	0.30, <0.01
<i>Sulfonates</i>	
PFBS (4C)	0.72
PFHxS (6C)	>0.99, >0.99
PFOS (8C)	<0.01, <0.01, >0.99

96

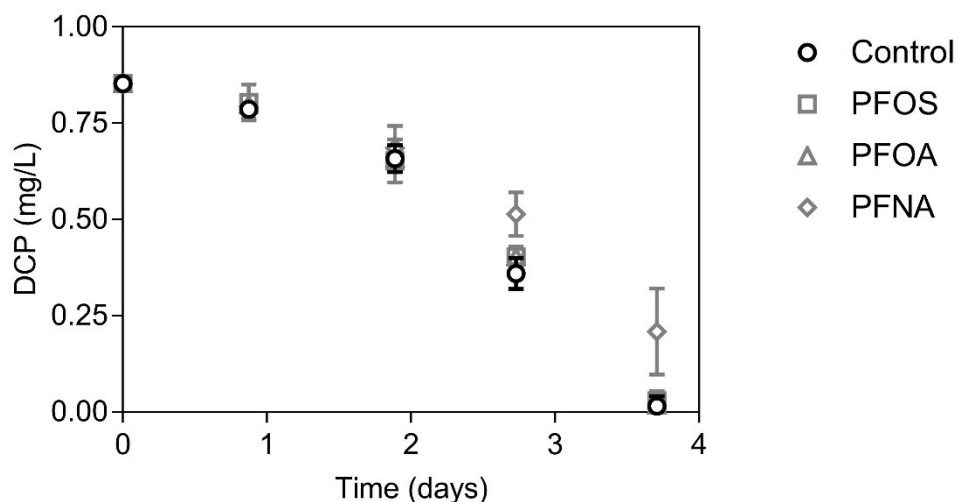
97

98 Figure SI.4. shows the degradation of 2,4-dichlorophenol (DCP) over time in no-PFAS  
99 control treatments and in treatments amended with 50 mg/L of various PFAS. The figure shows  
100 the average from triplicate microcosms; the error bars show the standard deviation of triplicates.  
101 This data was fit with the Gompertz model to determine the lag period prior to DCP degradation.  
102 Panels A and B show data obtained in experiments performed on two different dates.



103  
 104 **Figure SI.4. Degradation of 2,4-dichlorophenol (DCP) in the no-PFAS added control and in the presence of 50**  
 105 **mg/L of varying PFAS. Panel A. shows data from treatments amended with PFBA, PFBS, and PFHxS, and**  
 106 **Panel B. shows data from treatments amended with PFOS, PFOA, and PFNA. The data on these two panels**  
 107 **was obtained from experiments performed on different days.**  
 108

109 Figure SI.5. shows the degradation of DCP over time in no-PFAS control treatments and  
 110 in treatments amended with 5 mg/L of PFOS, PFOA, and PFNA. The figure shows the average  
 111 of data from triplicate microcosms and the error bars show the standard deviation of those data.  
 112 This data was fit with the Gompertz model to determine the lag period prior to DCP degradation.  
 113 This experiment was performed on a different date than the experiments shown in Figure SI.4.  
 114



115  
 116 **Figure SI.5. Degradation of DCP in no-PFAS added control treatments and in treatments amended with 5**  
 117 **mg/L of either PFOS, PFOA, or PFNA. The average of triplicate treatments are shown with error bars**  
 118 **showing the standard deviation.**

119  
 120 Figure SI.6. shows the clustering of the samples based on the beta diversity between  
 121 samples, as determined by Bray Curtis. The Illumina analysis was performed on samples taken  
 122 on Day 1 and Day 25 (the end of the experiment) of the DCP-degradation experiment. The initial  
 123 samples clustered together and then shifted as a result of time and PFAS exposure. The AFFF  
 124 samples clustered apart from the other samples. Two controls and one PFHxS+PFOS samples  
 125 also clustered separately. The Kruskal-Wallis test was used to determine if any OTUs with a  
 126 relative abundance above 0.5% were statistically different between the treatments; none were.  
 127 The largest difference between the three samples that were most different from the others (two  
 128 controls and one PFOS+PFHxS) was the high abundance of a *Clostridia* OTU and the lower  
 129 abundance of an *Anaerolinea* OTU (Figure SI.6)

130

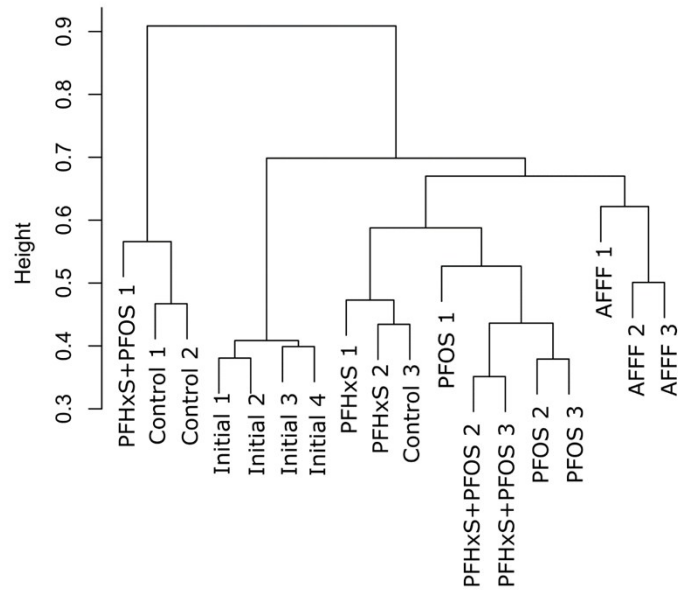
131

132

133

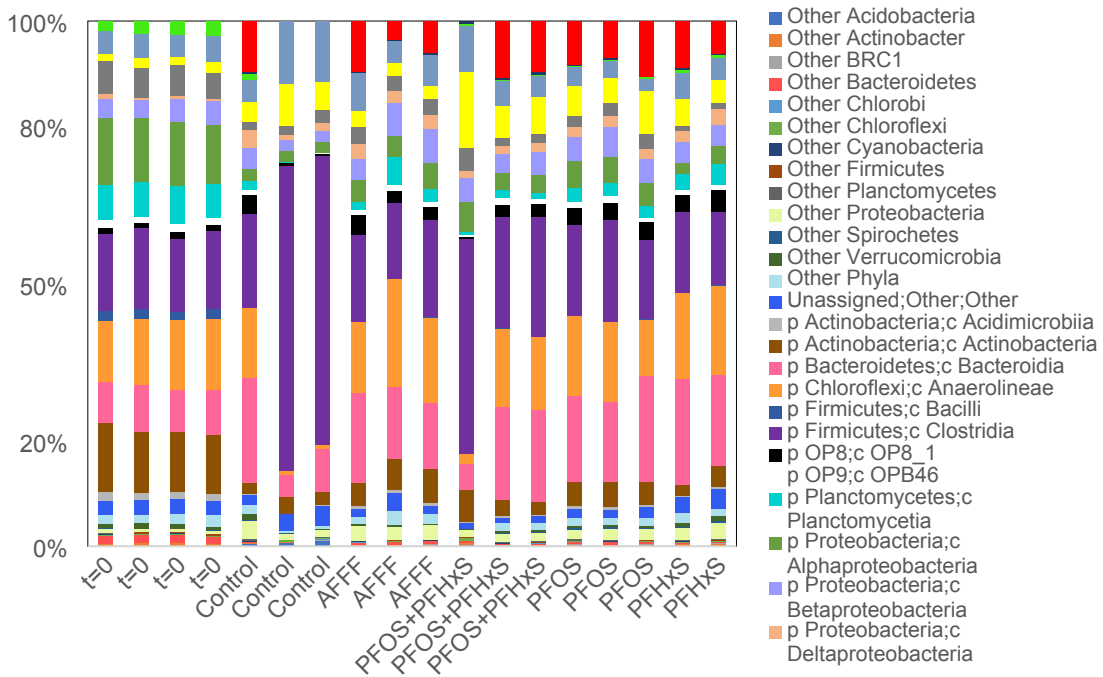


A.



134

B.



135

136 **Figure SI.6. Microbial community analysis from the DCP-degradation experiments. Panel A shows**  
 137 **hierarchical clustering of samples based on Bray Curtis beta diversity analysis. Panel B shows the relative**  
 138 **abundance of the 16S rRNA gene sequences at the Class phylogenetic level for the initial and each of the**  
 139 **treatments. Specific Classes that were present at less than 1% were lumped at the Phylum phylogenetic level.**  
 140 **Phyla present at less than 1% were also lumped together.**  
 141

142 Table SI.2. shows the chemical oxygen demand (COD) (mg/L) in no-PFAS control  
 143 treatments, treatments amended with PFAS only or with DCP+PFAS. The time zero  
 144 measurement was taken of the initial diluted digester culture prior to the addition of PFAS and/or  
 145 DCP. The measurements taken on Day 3 were from the microcosms to which no DCP was  
 146 added. The measurements taken on Day 25 were from the microcosms to which DCP was added.  
 147 These data show the large COD added with the AFFF that was not present in the other  
 148 treatments.

149

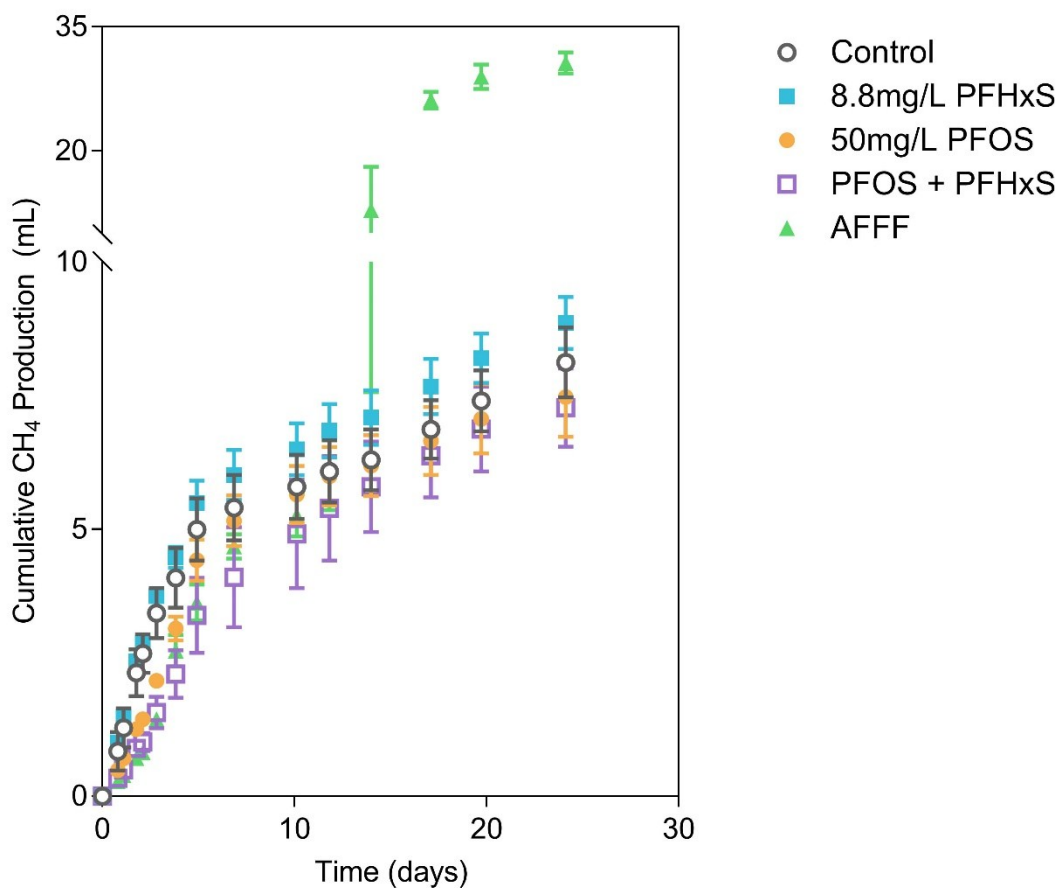
150 **Table SI.2. Chemical oxygen demand (COD) (mg/L) in no-PFAS controls and in treatments amended with**  
 151 **PFAS only or PFAS+DCP. The t=0 measurement was from the diluted digester culture. The t=3**  
 152 **measurements were taken from treatments that did not contain DCP. The t=25 measurements were taken**  
 153 **from treatments amended with DCP.**

154

	Day		
	0	3	25
<b>Control</b>	391.5	319.0	203.3
<b>AFFF as 50 mg/L PFOS</b>	391.5	2,681.3	1,339.6
<b>PFOS + PFHxS</b>	391.5	585.3	216.7
<b>50 mg/L PFOS</b>	391.5	583.3	226.0
<b>8.8 mg/L PFHxS</b>	391.5	321.3	207.3

155

156 Figure SI.7. shows the methane production over time in the DCP-degradation  
 157 experiments. Data from no-PFAS control treatments and treatments amended with 50 mg/L  
 158 PFOS, 8.8 mg/L PFHxS, PFOS (50 mg/L)+PFHxS (8.8 mg/L), and AFFF is shown. The figure  
 159 shows the average of data from triplicate microcosms and the error bars show the standard  
 160 deviation of those data. This data also shows the extra methane production that occurred in the  
 161 AFFF-amended treatments. This rapid increase in methane production was observed after the  
 162 initial COD present in the diluted digester culture appeared to be degraded (on about Day 25),  
 163 presumably a result of the large COD amended to the microcosms as part of the AFFF.



164

165 **Figure SI.7. Methane production in treatments used to determine the effect of AFFF and its major PFAS**  
 166 **constituents on the degradation of 2,4-dichlorophenol (DCP).**

167

## 168 REFERENCES

- 169 1. Nelson DK, Lapara TM, Novak PJ. Effects of Ethanol-based Fuel Contamination: Microbial Community  
 170 Changes, Production of Regulated Compounds, and Methane Generation. *Environ Sci Technol.*  
 171 2010;44(12):4525–30.
- 172 2. Nelson DK, Lapara TM, Novak PJ. Structure and Function of Assemblages of Bacteria and Archaea in  
 173 Model Anaerobic Aquifer Columns: Can Functional Instability Be Practically Beneficial? *Environ Sci*  
 174 *Technol.* 2012;46:10137–44.
- 175 3. Hook SE, Northwood KS, Wright AG, McBride BW. Long-Term Monensin Supplementation Does Not  
 176 Significantly Affect the Quantity or Diversity of Methanogens in the Rumen of the Lactating Dairy Cow.  
 177 *Appl Environ Microbiol.* 2009;75(2):374–80.  
 178